NASA TECHNICAL MEMORANDUM

NASA TM X-3411

NASA TM X-3411

CASE FILE COPY

EXPERIMENTAL EFFECTS OF FUSELAGE CAMBER ON LONGITUDINAL AERODYNAMIC CHARACTERISTICS OF A SERIES OF WING-FUSELAGE CONFIGURATIONS AT A MACH NUMBER OF 1.41

Samuel M. Dollyhigh, Odell A. Morris, and Mary S. Adams

Langley Research Center
Hampton, Va. 23665

NATIONAL AERONAUTICS AND SPACE ADMINISTRATION • WASHINGTON, D. C. • OCTOBER 1976

1. Report No.	2. Government Accession No.	3. Recipient's Catalog No.
NASA TM X-3411		

4. Title and Subtitle	5. Report Date
EXPERIMENTAL EFFECTS OF FUSELAGE CAMBER ON LONGITUDINAL AERODYNAMIC CHARACTERISTICS OF A SERIES OF WING-FUSELAGE CONFIGURATIONS AT A MACH NUMBER OF 1.41	October 1976
	6. Performing Organization Code
7. Author(s)	8. Performing Organization Report No.
Samuel M. Dollyhigh, Odell A. Morris, and Mary S. Adams	L-10847
9. Performing Organization Name and Address	10. Work Unit No.
NASA Langley Research Center Hampton, VA 23665	505-11-21-04
	11. Contract or Grant No.
	13. Type of Report and Period Covered
12. Sponsoring Agency Name and Address	Technical Memorandum
National Aeronautics and Space Administration Washington, DC 20546	14. Sponsoring Agency Code

15. Supplementary Notes

16. Abstract

An experimental investigation has been conducted to evaluate a method for the integration of a fighter-type fuselage with a theoretical wing to preserve desirable wing aerodynamic characteristics for efficient maneuvering. The investigation was conducted by using semispan wing-fuselage models mounted on a splitter plate. The models were tested through an angle-of-attack range at a Mach number of 1.41. The wing had a leading-edge sweep angle of 50° and an aspect ratio of 2.76; the wing camber surface was designed for minimum drag due to lift and was to be self-trimming at a lift coefficient of 0.2 and at a Mach number of 1.40. Previous experience had indicated that the self-trimming feature of the wing is extremely sensitive to the integration of the theoretical wing with the fuselage. A series of five fuselages of various camber was tested on the wing.

17. Key Words (Suggested by Author(s))	18. Distribution Statement
Aircraft design Supersonic design Wind-tunnel testing	Unclassified - Unlimited Subject Category 01

19. Security Classif. (of this report)	20. Security Classif. (of this page)	21. No. of Pages	22. Price*
Unclassified	Unclassified	25	$3.75

* For sale by the National Technical Information Service, Springfield, Virginia 22161

EXPERIMENTAL EFFECTS OF FUSELAGE CAMBER ON LONGITUDINAL AERODYNAMIC CHARACTERISTICS OF A SERIES OF WING-FUSELAGE CONFIGURATIONS AT A MACH NUMBER OF 1.41

Samuel M. Dollyhigh, Odell A. Morris,
and Mary S. Adams
Langley Research Center

SUMMARY

An experimental investigation has been conducted to evaluate a method for the integration of a fighter-type fuselage with a theoretical wing to preserve desirable wing aerodynamic characteristics for efficient maneuvering. The investigation was conducted by using semispan wing-fuselage models mounted on a splitter plate. The models were tested through an angle-of-attack range at a Mach number of 1.41. The wing had a leading-edge sweep angle of 50° and an aspect ratio of 2.76; the wing camber surface was designed for minimum drag due to lift and was to be self-trimming at a lift coefficient of 0.2 and at a Mach number of 1.40. Previous experience had indicated that the self-trimming feature of the wing is extremely sensitive to the integration of the theoretical wing with the fuselage. A series of five fuselages of various camber was tested on the wing.

The results showed a complete loss of the self-trimming feature of the wing with the addition of an uncambered fuselage; however, a trimmed lift coefficient over twice that desired resulted when the fuselage was cambered to follow the camber line of the theoretical wing root section. The other three fuselages were cambered in such a way that any longitudinal change in fuselage cross-sectional area was distributed equally above and below the

theoretical wing camber surface. This method of integrating the fuselage was chosen because it had been used successfully on supersonic transport configurations at higher Mach numbers and lower design lift coefficients. The results show that this method of cambering the fuselage is also applicable to fighter-type configurations at lower supersonic Mach numbers.

Baseline or reference-point data are presented in the appendix. These data are for an uncambered wing of the same planform and thickness distribution and with uncambered fuselages.

INTRODUCTION

As part of a research program to advance fighter technology, the National Aeronautics and Space Administration has undertaken research related to highly maneuverable fighters. At supersonic speeds, there is generally a problem sustaining the high turn rates that fighters are aerodynamically capable of achieving. This condition is usually the result of high drag associated with the lift coefficients that are required for maneuverability. For a typical aft-horizontal tail fighter, the drag due to trimming the aircraft accounts for much of the total drag because of increased longitudinal stability at supersonic speeds. In this paper, consideration is given to a means of lowering the supersonic trim drag without sacrificing inherent longitudinal stability at any Mach number.

The wing design procedure presented in reference 1 provides a method to design wings that have a minimum drag for a given lift and a zero pitching moment about a given reference point. Previous experience (refs. 2 and 3) has indicated that the integration of the fuselage with the wing is extremely sensitive. The desired aerodynamic characteristics designed into the wing, especially the self-trimming feature, could be either lost or overridden by the addition of a fuselage.

Earlier research performed on this problem for supersonic transport-type wings was reported in references 4 and 5. For fighters, however, the problem was suspected to be more acute because the fuselage is generally larger relative to the wing planform and the wing is designed for a higher lift coefficient; both these conditions necessitate more wing camber for a fighter. This report presents the results of an investigation into the problem of cambering a fuselage to preserve the desired aerodynamic characteristics of a typical fighter wing. The wing had a leading-edge sweep angle of 50° and an aspect ratio of 2.76; the wing camber surface was designed for minimum drag due to lift and was to be self-trimming at a lift coefficient of 0.2 and at a Mach number of 1.40. Five fuselages of various camber were integrated with the wing; they were bodies of revolution with a cross-sectional area distribution typical of an equivalent cross-sectional area distribution of a single-engine fighter. Wind-tunnel tests of the five wing-bodies were conducted in the Langley 4-foot supersonic pressure tunnel at a Mach number of 1.41.

Also presented is an appendix which contains data for two straight fuselages on an uncambered wing of the same planform and thickness distribution. One fuselage was area-ruled with respect to the wing while the other was not. These data were taken to determine the accuracy of the test technique and are presented in this paper to serve as a baseline for the effects of both wing and body camber.

SYMBOLS

The force and moment coefficients are referenced to the stability axis system. The moment reference point was located at fuselage station 53.39 cm ($0.40\bar{c}$).

A cross-sectional area, cm^2

b span, cm

C_D drag coefficient, $\frac{\text{Drag}}{qS}$

C_L lift coefficient, $\frac{\text{Lift}}{qS}$

$C_{L,des}$ design lift coefficient

C_m pitching-moment coefficient, $\frac{\text{Pitching moment}}{qS\bar{c}}$

c streamwise chord, cm

c_r theoretical root chord of wing

$\bar{c}$ mean aerodynamic chord, cm

L/D lift-drag ratio

M free-stream Mach number

q free-stream dynamic pressure, Pa

r body radius, cm

S reference area of wing including fuselage interrupt

x longitudinal distance, positive rearward from nose, cm

x_c longitudinal distance, positive rearward from leading edge of wing, cm

y lateral distance from center line of airplane, cm

z vertical ordinate, positive up, cm

z_c wing camber ordinate with respect to leading edge of wing, cm

α angle of attack, deg

DESCRIPTION OF MODEL AND INSTRUMENTATION

A planform drawing of the model is shown in figure 1. The wing planform was a clipped arrow with a leading-edge sweep angle of 50° and an aspect ratio of 2.76. The taper ratio of the theoretical planform was 0.20 and the notch ratio was 0.157. The streamwise airfoil thickness distribution was that of an NACA 65A004.5 airfoil. The wing had a camber surface that was designed for minimum drag due to lift at a Mach number M of 1.4 and a lift coefficient C_L of 0.2 by the method of reference 1. The camber surface was also designed so that the wing would be self-trimming about a center of gravity at 40 percent of the mean aerodynamic chord. The wing camber surface ordinates are given in table I and are shown in figure 2.

Five fuselages were integrated with the wing. Fuselage radii and center-line camber ordinates are given in table II for the five fuselages tested. Profile drawings of the five fuselages are shown in figure 3. The camber line of the theoretical wing root section is shown inside each of the fuselages at its proper location with respect to the body. All the fuselages were designed from the same basic body, which was an uncambered body with a Sears-Haack nose, followed by a constant area body (same radii as the straight body that was not area-ruled in the appendix). All the fuselages were area ruled and all except fuselage 1 were cambered to form the five fuselages tested. The design point for area rule and camber was $M = 1.4$ and $C_L = 0.2$. The fuselages were area-ruled by the method of reference 6 so as to account for the different body cambers with respect to the wing. Fuselage 1 was not cambered, whereas fuselage 2 had the greatest camber which was equal to the theoretical root-section camber of the wing. Following the method presented in references 1 and 5, fuselages 3 to 5 were cambered so that the longitudinal rates of area change above and below the wing camber surface were equal. Fuselages 3, 4, and 5 had 10.0, 50.0, and 65.0 percent, respectively, of the cross-sectional area above the wing camber surface at approximately the quarter-chord of the root section. For this particular wing, 65.0 percent of the area above the wing camber surface at the root quarter-chord was as low as the wing could be placed with respect to the fuselage and still satisfy the equal-area-change requirement without placing the theoretical wing outside the fuselage. In general, because of the nature of supersonic camber surfaces (fig. 2) designed by the method of reference 1, any low-wing configuration would be difficult to camber by the equal-area-change method.

Each of the five fuselages was constructed as a half-body of wood and was attached to a half-span steel wing. The wing was in turn mounted on a four-component balance housed within the splitter plate. A clearance of 0.03 to 0.05 cm was maintained between the wing and the splitter plate. The wing and the plate moved through an angle-of-attack range as a unit. In order to avoid flow disturbances where the half-body extended beyond the leading edge of the splitter plate, a mirror image of this portion of the body was mounted to the back surface of the splitter plate. The small gap was maintained between these half-bodies so that the proper forces and moments were measured.

TESTS AND CORRECTIONS

The tests were conducted in the Langley 4-foot supersonic pressure tunnel at a Mach number of 1.41, at a stagnation temperature of 317 K, and at a stagnation pressure of 70 878 Pa. The tests were conducted at a Reynolds number per meter of 9.84×10^6. The dewpoint was held sufficiently low to prevent measurable condensation effects in the test section. Tests were made through an angle-of-attack range of approximately -4° to 10° or to as high an angle as balance load limits permitted. The body base pressures were measured and the drag forces were adjusted to correspond to the condition of free-stream static pressure at the base of the model. In order to insure boundary-layer transition to turbulent flow, 0.16-cm-wide transition strips of No. 60 carborundum grit were applied 1.02 cm streamwise on the wing and 2.54 cm aft of the nose on the fuselage. The transition strips are shown to be adequate, according to the method of reference 7.

DISCUSSION OF RESULTS

The analytical method of reference 1 was used to design the wing camber surface. The numerical method, which is based on linearized theory, calculates a camber surface that will support an optimum lifting-pressure distribution at a specified lift coefficient and Mach number. The method does not consider thickness pressures; therefore, an airfoil thickness distribution is preselected and is distributed symmetrically about the camber surface. For the exposed wing, this distribution is not a problem since the wing thickness ratio is primarily constrained by considerations of wave drag, structural weight, wing fuel volume, and landing-gear location. However, the separation of drag due to volumetric displacement of the body and the wing and drag due to lift is of greater concern when the fuselage is integrated with the theoretical wing design. References 4 and 5 cover previous work at Mach number 2.0 or higher in the integration of a fuselage and wing for a transport-type configuration. In these references, the wing design loading distribution was found to be essentially unchanged if the change in fuselage cross-sectional area was distributed equally above and below the wing camber surface. More explicitly, the change in cross-sectional area with length ($\partial A/\partial x$) above and below the wing camber surface must be the same for each fuselage station. Although this method does not strictly adhere to a symmetrical local thickness about a wing camber surface, it was found to give satisfactory results. Fighter-type aircraft, however, tend to have larger fuselages relative to wing planform area than transports; thus, a greater percentage of the theoretical wing planform is covered. Fighters also tend to need greater fuselage camber than transports because the wing is more highly cambered due to the requirement for higher lift coefficients. The applicability of the area-balancing method to fighter-type configurations at a more pertinent Mach number for fighters is investigated in this paper. As part of the program, a computer code has been written that cambers the fuselage with respect to the wing camber surface. Since the equation to be satisfied

$$\left(\frac{\partial A}{\partial x}\right)_{\text{below}} = \left(\frac{\partial A}{\partial x}\right)_{\text{above}}$$

does not have a sense of direction, a key station is designated and the wing position or a percent cross-sectional area is specified and the remaining fuselage stations are sheared to result in the desired fuselage camber. Interactive graphics are incorporated via a cathode ray tube so that a visual check of the results is available. In this process, the operator may intervene if the results are not satisfactory or if the rate of longitudinal area change cannot be balanced about the wing camber surface. The operator has the option of either changing the initial conditions and restarting at the original key station or designating a troublesome station as the key station and proceeding. For the fuselages tested in this investigation, the key station was designated to be the quarter-chord of the root section and the fuselages were then cambered by using the computer code. Fuselages 3, 4, and 5 were cambered so that the wing-fuselage intercept was in the high, mid, and low position, respectively. In the low-wing position, difficulty is generally encountered in achieving the proper distribution of cross-sectional area because the trailing edge of the root camber line tends to lie outside the fuselage.

Sixty-five percent of the cross-sectional area above the wing camber plane at the root quarter-chord was as low as the wing could be placed without encountering a problem at the trailing edge of the wing. A look at the spanwise slopes of the wing camber surface (fig. 2) will show why this is true. Figure 2 shows in nondimensional form the camber surface of the wing with respect to the leading edge (i.e., leading edge at $z_c = 0.0$).

The data in figure 4 bracket the extremes in integrating a fuselage with a wing camber surface. Also shown are aerodynamic data for the wing alone, for an uncambered fuselage (fuselage 1), for a fuselage with 50 percent of the area distributed above the wing camber plane (fuselage 4), and for a fuselage that follows the wing-root camber line (fuselage 2). The pitching-moment data show that the combination of fuselage 4 and wing has a value of C_m close to that of the trim lift coefficient of the wing alone. The trim lift coefficients of fuselages 1 and 2 are approximately 0.25 below and above the design lift coefficient, respectively. Although fuselage 1 has a little less drag than fuselage 4, it is not trimmed and, as pointed out earlier, a trim drag penalty would be required.

Figure 5 shows the effect of moving the wing, either up or down, with respect to the body. Fuselages 3 to 5 have all been cambered such that the longitudinal rate of area change is distributed about the wing camber surface. There are some changes in pitching moment and drag due to the high position of the wing (i.e., fuselage-3—wing configuration with 10 percent of fuselage cross-sectional area above the wing camber surface at root quarter-chord has a slightly higher drag and pitching moment than the other combinations). The low-wing (65 percent of the area above the wing camber surface at root quarter-chord) configuration was essentially unchanged from the mid-wing (50 percent of the area above the wing camber surface at root quarter-chord) configuration in longitudinal aerodynamic characteristics. This difference between the high-wing configuration and the other two is an indication of the high sensitivity in pitching moment to fuselage camber. The high-wing position results in a slightly greater net displacement of the fuselage center line. The greater displacement is a result of both the severe spanwise slopes in wing camber as the trailing edge is approached and the fact that most of the change in area above the wing camber surface is due to area rule. A significant amount of cross-sectional area above the wing that is not involved in keeping

$$\left(\frac{\partial A}{\partial x}\right)_{above} = \left(\frac{\partial A}{\partial x}\right)_{below}$$

tends to modulate the fuselage camber somewhat in the regions of severe spanwise slopes in wing camber. A look at the spanwise camber surface near the trailing edge of the wing in figure 2 will show why this is so. The high-wing body camber slightly overshoots and then rises as the cross-sectional area increases. Although the wing-fuselage closely approximates the desired characteristics, there is apparently an oversensitivity in the extremes when the area either above or below the wing camber surface is approximately the same as the area that is added or substracted due to area rule.

CONCLUDING REMARKS

An experimental investigation has been conducted to evaluate a method for the integration of a fighter-type fuselage with a theoretical wing to preserve desirable wing aerodynamic characteristics for efficient maneuvering. The investigation was conducted by using semispan wing-fuselage models mounted on a splitter plate. The models were tested through an angle-of-attack range at a Mach number of 1.41. The wing had a leading-edge sweep angle of 50° and an aspect ratio of 2.76; the wing camber surface was designed for minimum drag due to lift and was to be self-trimming at a lift coefficient of 0.2 and at a Mach number of 1.40. Previous experience has indicated that the self-trimming feature of a wing is extremely sensitive to the integration of the theoretical wing with the fuselage. A series of five fuselages of various camber was tested on the wing.

The results showed a complete loss of the self-trimming feature of the wing with the addition of an uncambered fuselage; however, a trimmed lift coefficient over twice that desired resulted when the fuselage was cambered to follow the camber line of theoretical wing root section. The other three fuselages were cambered in such a way that any longitudinal change in fuselage cross-sectional area was distributed equally above and below the theoretical wing camber surface that was enclosed by the fuselage. The three fuselages cambered by this method had the amount of cross-sectional area above the wing camber surface at approximately the root quarter-chord varied so as to form a series of high-, mid-, and low-wing configurations. All three of these configurations were self-trimming at approximately the design point of the wing alone. However, there was an indication of oversensitivity in fuselage camber if the wing was placed extremely high or low so that the area above or below the wing camber surface is approximately the same as the area that is added or subtracted because of area rule.

Langley Research Center
National Aeronautics and Space Administration
Hampton, VA 23665
August 3, 1976

APPENDIX

DISCUSSION OF UNCAMBERED FUSELAGES

Preliminary to designing the five cambered fuselages, two uncambered fuselages were tested on an uncambered wing with plan-form and thickness distribution identical to the cambered wing used in this investigation. One fuselage was area-ruled with respect to the wing and the other was not. The body radii for these two bodies are given in the following table:

x, cm	r, (Not area-ruled), cm	r, (Area-ruled), cm	x, cm	r, (Not area-ruled), cm	r, (Area-ruled), cm
0	0	0	36.491	3.912	3.513
.508	.302	.302	39.106	3.912	3.259
1.016	.505	.505	41.712	3.912	3.068
1.524	.683	.683	44.318	3.912	2.918
2.032	.841	.841	46.927	3.912	2.852
2.540	.988	.988	49.533	3.912	2.847
3.810	1.318	1.318	52.141	3.912	2.896
5.08	1.608	1.608	54.747	3.912	2.992
7.62	2.103	2.103	57.353	3.912	3.129
10.16	2.517	2.517	59.962	3.912	3.264
12.70	2.863	2.863	62.568	3.912	3.391
15.24	3.152	3.152	65.242	3.912	3.510
17.78	3.391	3.391	67.782	3.912	3.627
20.32	3.581	3.581	70.388	3.912	3.713
22.86	3.726	3.726	72.994	3.912	3.790
25.40	3.830	3.830	76.602	3.912	3.843
27.94	3.891	3.891	78.209	3.912	3.884
30.48	3.912	3.912	80.817	3.912	3.909
33.891	3.912	3.744	81.280	3.912	3.912

The fuselage that was not area-ruled served as a baseline from which all the fuselages were derived by either area rule or area rule and camber.

Model construction and test conditions were identical to those used for the cambered fuselages. These data were taken to check the reliability of the testing technique by using the semispan model mounted on a splitter plate. A drag reduction of 0.0020 was calculated by the method of reference 6 and was experimentally realized for the effect of the area-ruled body at a Mach number of 1.40. This agreement is interpreted to indicate that the test technique is reliable. These data are presented in figure 6 and serve as a baseline for the effects of both wing and body camber.

REFERENCES

1. Sorrells, Russell B.; and Miller, David S.: Numerical Method for Design of Minimum-Drag Supersonic Wing Camber With Constraints on Pitching Moment and Surface Deformation. NASA TN D-7097, 1972.
2. Dollyhigh, Samuel M.: Subsonic and Supersonic Longitudinal Stability and Control Characteristics of an Aft Tail Fighter Configuration With Cambered and Uncambered Wings and Uncambered Fuselage. NASA TM X-3078, 1974.
3. Dollyhigh, Samuel M.: Wing-Camber Effects on Longitudinal Aerodynamic Characteristics of a Variable-Sweep Fighter Configuration at Mach Numbers From 1.60 to 2.86. NASA TM X-2826, 1973.
4. Baals, Donald P.; Robins, A. Warner; and Harris, Roy V., Jr.: Aerodynamic Design Integration of Supersonic Aircraft. AIAA Paper No. 68-1018, Oct. 1968.
5. Carlson, Harry W.: Longitudinal Aerodynamic Characteristics at Mach Number 2.02 of a Series of Wing-Body Configurations Employing a Cambered and Twisted Arrow Wing. NASA TM X-838, 1963.
6. Harris, Roy V., Jr.: An Analysis and Correlation of Aircraft Wave Drag. NASA TM X-947, 1964.
7. Braslow, Albert L.; Hicks, Raymond M.; and Harris, Roy V., Jr.: Use of Grit-Type Boundary-Layer-Transition Trips on Wind-Tunnel Models. NASA TN D-3579, 1966.

TABLE I.- CAMBER SURFACE ORDINATES

[Wing sections were sheared so that x/c = 0.25 was at z = 0.0 in model reference axis]

x/c	$\frac{z_c}{c}$, in percent, with respect to leading edge at $\frac{y}{b/2}$ of -														
	0	0.02	0.04	0.06	0.08	0.10	0.12	0.200	0.300	0.400	0.500	0.600	0.700	0.800	0.900	1.000
0	0	0	0	0	0	0	0	0	0	0	0	0	0	0	0
.05	-.732	-.331	-.235	-.194	-.164	-.134	-.027	.253	.313	.360	.400	.451	.521	.365	.316	.328
.10	-1.951	-.976	-.712	-.582	-.487	-.408	-.272	.389	.513	.612	.697	.795	.888	.799	.809	.840
.15	-3.292	-1.732	-1.303	-1.067	-.907	-.783	-.606	.459	.656	.810	.942	1.067	1.199	1.148	1.155	1.383
.20	-4.683	-2.558	-1.945	-1.616	-1.387	-1.204	-.987	.485	.759	.962	1.137	1.307	1.468	1.445	1.518	1.988
.25	-6.080	-3.415	-2.626	-2.198	-1.900	-1.666	-1.409	.474	.829	1.096	1.311	1.521	1.723	1.742	1.636	2.593
.30	-7.471	-4.278	-3.325	-2.799	-2.433	-2.147	-1.845	.442	.884	1.203	1.475	1.711	1.950	2.005	2.134	3.198
35	-8.831	-5.147	-4.037	-3.407	2.978	-2.642	-2.301	.394	.921	1.301	1.608	1.890	2.163	2.250	2.409	3.833
.40	-10.154	-6.004	-4.736	-4.021	-3.524	-3.144	-2.764	.332	.943	1.381	1.741	2.057	2.362	2.479	2.684	4.469
.50	-12.652	-7.661	-6.116	-5.229	-4.615	-4.140	-3.683	.209	.978	1.523	1.976	2.367	2.747	2.936	3.212	5.740
.55	-13.822	-8.449	-6.777	-5.818	-5.148	-4.629	-4.139	.147	.992	1.584	2.078	2.510	2.862	3.148	3.443	6.406
.60	-14.923	-9.119	-7.413	-6.387	-5.661	-5.104	-4.588	.085	.998	1.646	2.180	2.653	3.089	3.343	3.674	7.042
.65	-15.957	-9.919	-8.023	-6.930	-6.160	-5.565	-5.017	.038	1.011	1.708	2.282	2.785	3.274	3.537	3.927	7.677
.70	-16.923	-10.594	-8.601	-7.447	-6.640	-6.013	-5.432	.010	1.033	1.770	2.384	2.916	3.431	3.731	4.137	8.313
.75	-17.815	-11.232	-9.148	-7.944	-7.094	-6.435	-5.834	-.042	1.055	1.840	2.476	3.047	3.589	3.926	4.346	8.979
.80	-18.628	-11.819	-9.663	-8.410	-7.521	-6.843	-6.215	-.068	1.084	1.902	2.578	3.179	3.746	4.120	4.555	9.614
.85	-19.366	-12.364	-10.133	-8.843	-7.922	-7.217	-6.576	-.071	1.123	1.973	2.681	3.310	3.903	4.298	4.742	10.250
.90	-20.02	-12.852	-10.572	-9.244	-8.297	-7.572	-6.916	-.067	1.169	2.053	2.783	3.430	4.046	4.475	4.929	10.916
.95	-20.597	-13.290	-10.968	-9.606	-8.646	-7.900	-7.229	-.041	1.223	2.142	2.895	3.561	4.203	4.652	5.094	11.552
1.00	-21.089	-13.677	-11.316	-9.935	-8.955	-8.201	-7.515	.000	1.293	2.231	3.008	3.693	4.361	4.830	5.260	12.187

TABLE II.- FUSELAGE RADII AND CENTER-LINE CAMBER ORDINATES

(a) Fuselage 1

x, cm	z, cm	r, cm
0	-1.313	0
.508		.302
1.016		.505
1.524		.683
2.032		.841
2.540		.988
3.810		1.318
5.08		1.608
7.62		2.103
10.16		2.517
12.70		2.863
15.24		3.152
17.78		3.391
20.32		3.581
22.86		3.726
25.40		3.830
27.94		3.891
30.48		3.912
33.02		3.810
35.56		3.612
38.10		3.381
40.64		3.147
43.18		3.025
45.72		2.964
48.26		2.911
50.80		2.858
53.34		2.951
55.88		3.058
58.42		3.183
60.96		3.315
63.50		3.439
66.04		3.556
68.58		3.645
71.12		3.724
73.66		3.790
76.20		3.840
78.74		3.879
81.28		3.912

(b) Fuselage 2

x, cm	z, cm	r, cm
0	2.316	0
.508		.302
1.016		.505
1.524		.683
2.032		.841
2.540		.988
3.810		1.318
5.08		1.608
7.62		2.103
10.16		2.517
12.70		2.863
15.24		3.152
17.78		3.391
20.32		3.581
22.86		3.726
25.40		3.830
27.94		3.891
30.48	1.918	3.912
33.02	1.290	3.744
35.56	.597	3.533
38.10	-.104	3.292
40.64	-.810	3.073
43.18	-1.481	2.936
45.72	-2.156	2.852
48.26	-2.725	2.860
50.80	-3.315	2.878
53.34	-3.813	2.979
55.88	-4.303	3.086
58.42	-4.717	3.208
60.96	-5.090	3.335
63.50	-5.423	3.454
66.04	-5.692	3.564
68.58	-5.718	3.650
71.12		3.726
73.66		3.790
76.20		3.840
78.74		3.879
81.28		3.912

(c) Fuselage 3

x, cm	z, cm	r, cm
0	0	0
.508		.302
1.016		.505
1.524		.683
2.032		.841
2.540		.988
3.810		1.318
5.08		1.608
7.62		2.103
10.16		2.517
12.70		2.863
15.24		3.152
17.78		3.391
20.32		3.581
22.86		3.726
25.40		3.830
27.94	-.018	3.891
30.48	-.287	3.912
33.02	-.597	3.754
35.56	-.973	3.508
38.10	-1.425	3.264
40.64	-1.941	3.020
43.18	-2.469	2.850
45.72	-3.155	2.802
48.26	-3.764	2.814
50.80	-4.041	2.870
53.34	-4.242	2.951
55.88	-4.366	3.066
58.42	-4.465	3.195
60.96	-4.539	3.332
63.50	-4.559	3.437
66.04	-4.483	3.520
68.58	-4.470	3.637
71.12		3.731
73.60		3.792
76.20		3.835
78.74		3.876
81.23		3.912

TABLE II.- Concluded

(d) Fuselage 4

x, cm	z, cm	r, cm
0	0.996	0
.508		.302
1.016		.505
1.524		.683
2.032		.841
2.540		.988
3.810		1.319
5.08		1.608
7.62		2.103
10.16		2.517
12.70		2.863
15.24		3.152
17.78		3.391
20.32		3.581
22.86		3.726
25.40		3.830
27.94		3.891
30.48	.927	3.912
33.02	.721	3.744
35.56	.432	3.523
38.10	.099	3.284
40.64	-.269	3.211
43.18	-.645	2.893
45.72	-1.016	2.794
48.26	-1.415	2.741
50.80	-1.763	2.794
53.34	-2.062	2.885
55.88	-2.337	3.005
58.42	-2.588	3.084
60.96	-2.799	3.297
63.50	-2.936	3.424
66.04	-2.974	3.536
68.58		3.647
71.12		3.736
73.66		3.805
76.20		3.848
78.74		3.884
81.28		3.912

(e) Fuselage 5

x, cm	z, cm	r, cm
0	1.336	0
.508		.302
1.016		.505
1.524		.683
2.032		.841
2.540		.988
3.810		1.318
5.08		1.608
7.62		2.103
10.16		2.517
12.70		2.863
15.24		3.152
17.78		3.391
20.32		3.581
22.86		3.726
25.40		3.830
27.94		3.891
30.48		3.912
33.02	1.204	3.739
35.56	.958	3.526
38.10	.668	3.299
40.64	.328	3.066
43.18	-.033	2.896
45.72	-.404	2.799
48.26	-.757	2.743
50.80	-1.110	2.797
53.34	-1.422	2.883
55.88	-1.732	3.015
58.42	-1.986	3.155
60.96	-2.223	3.299
63.50	-2.385	3.399
66.04	-2.449	3.533
68.58	-2.454	3.645
71.12		3.739
73.66		3.802
76.20		3.853
78.74		3.886
81.28		3.912

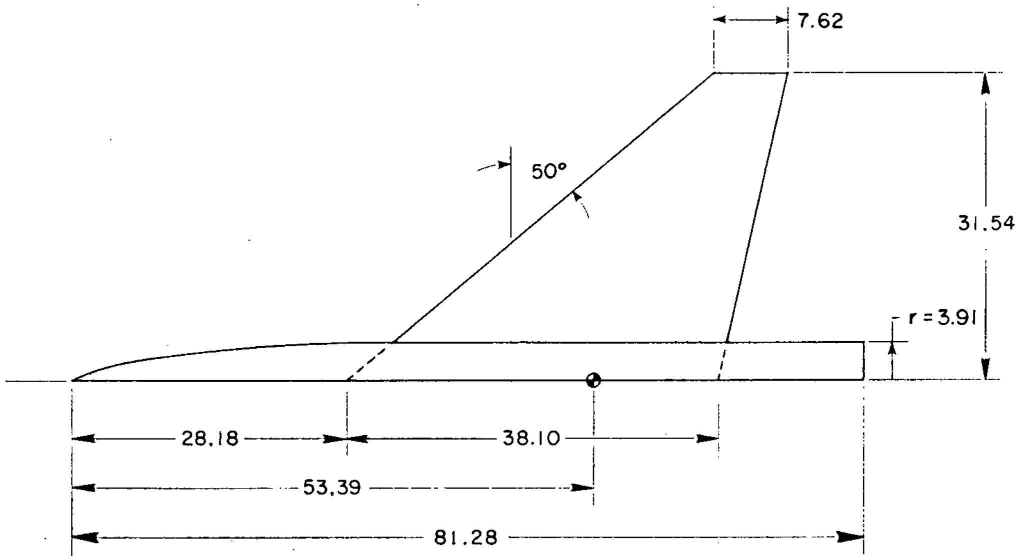

Figure 1.- Model planform. Dimensions are in centimeters.

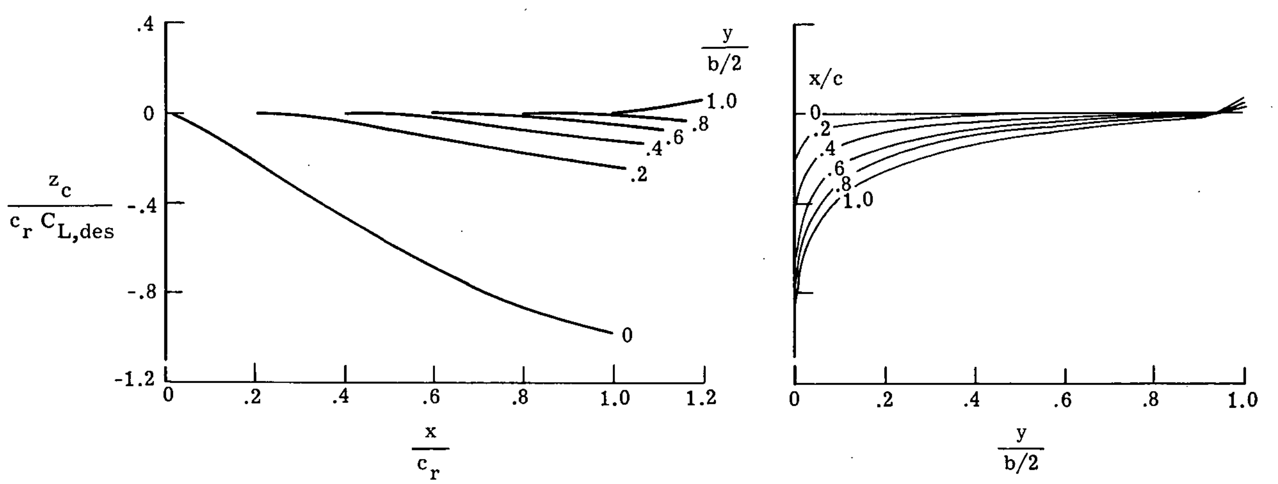

Figure 2.- Camber surface of wing with respect to leading edge.

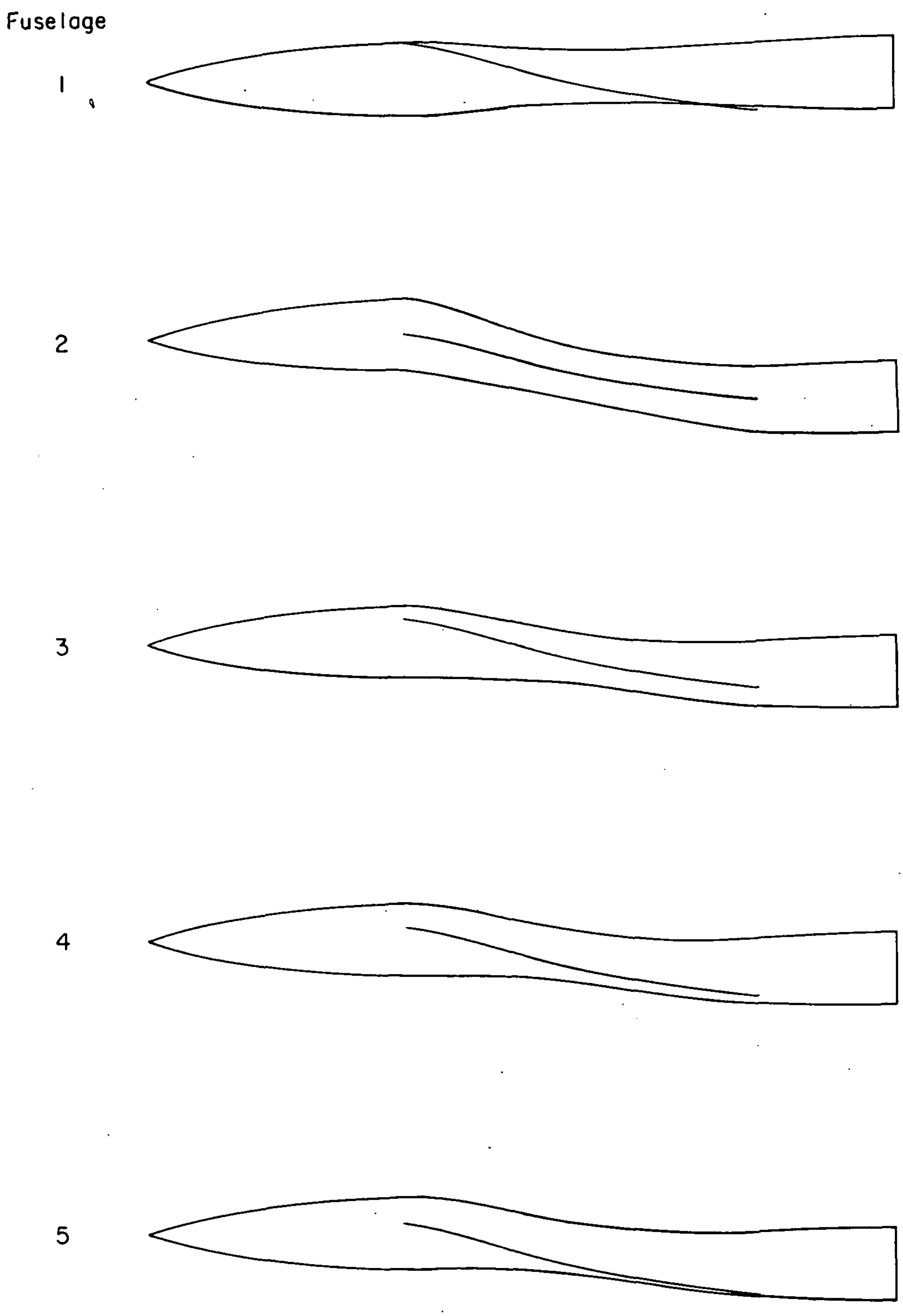

Figure 3.- Profile view of models. Line inside fuselage is theoretical camber line of wing root section.

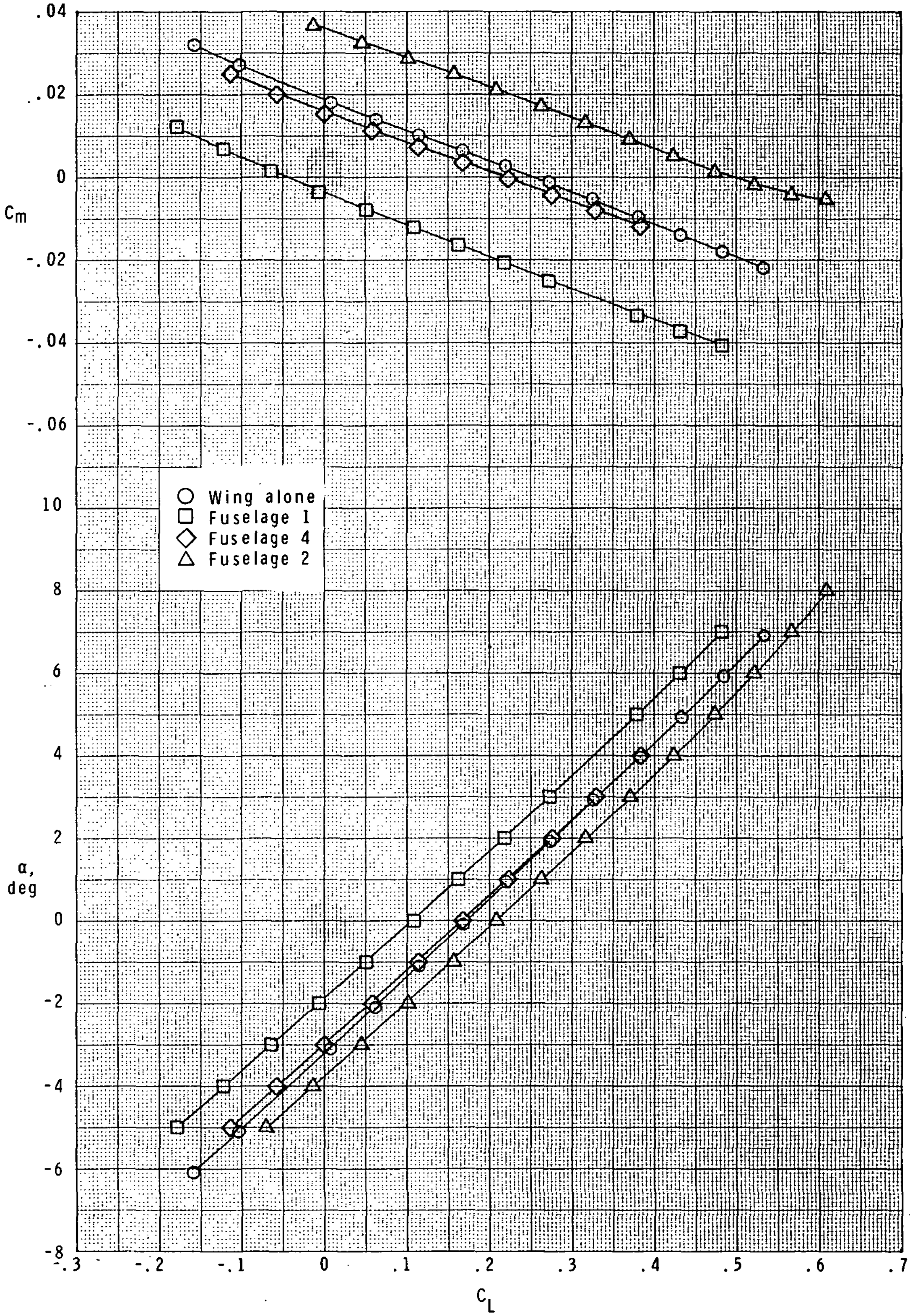

Figure 4.- Effect of fuselage camber.

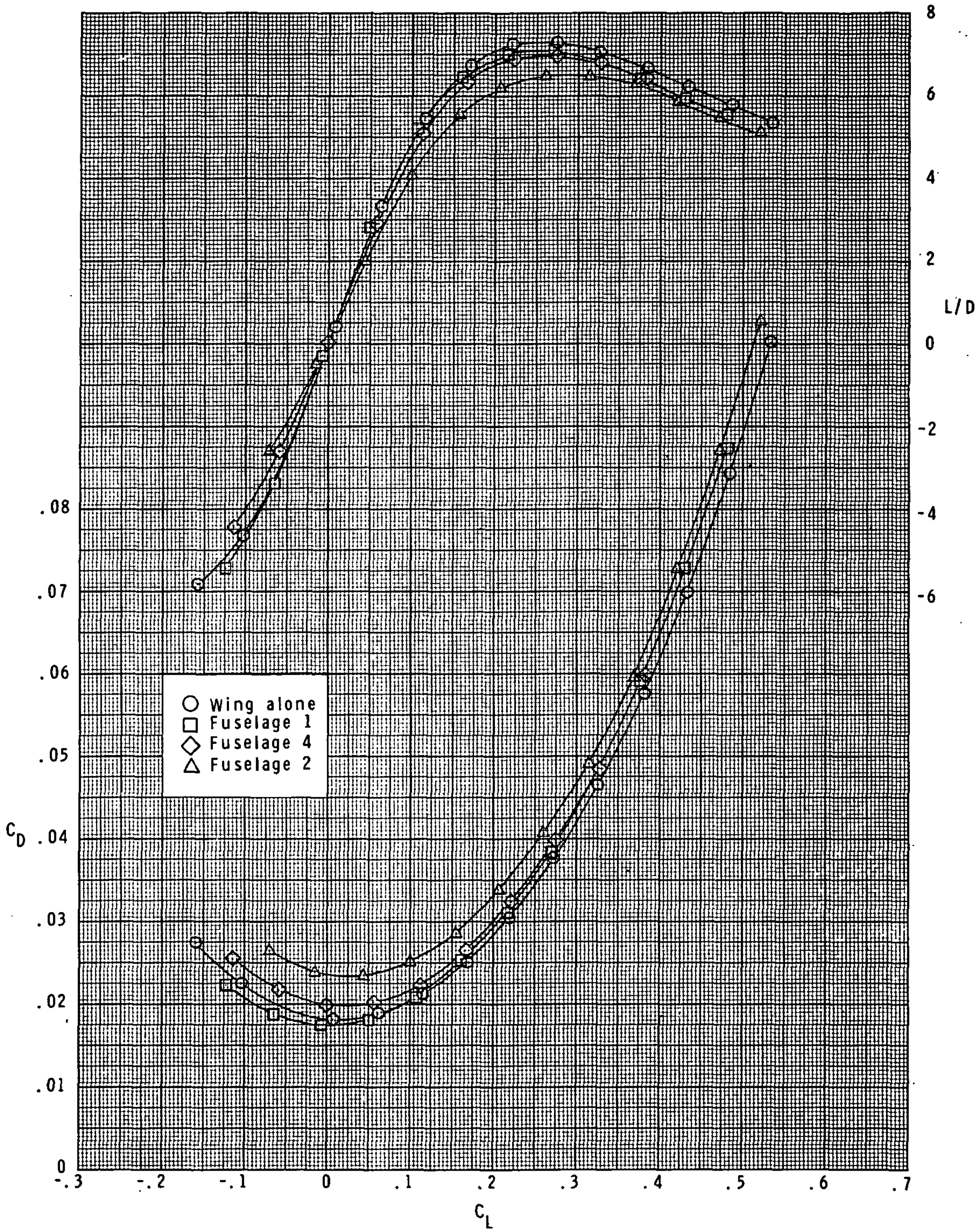

Figure 4.- Concluded.

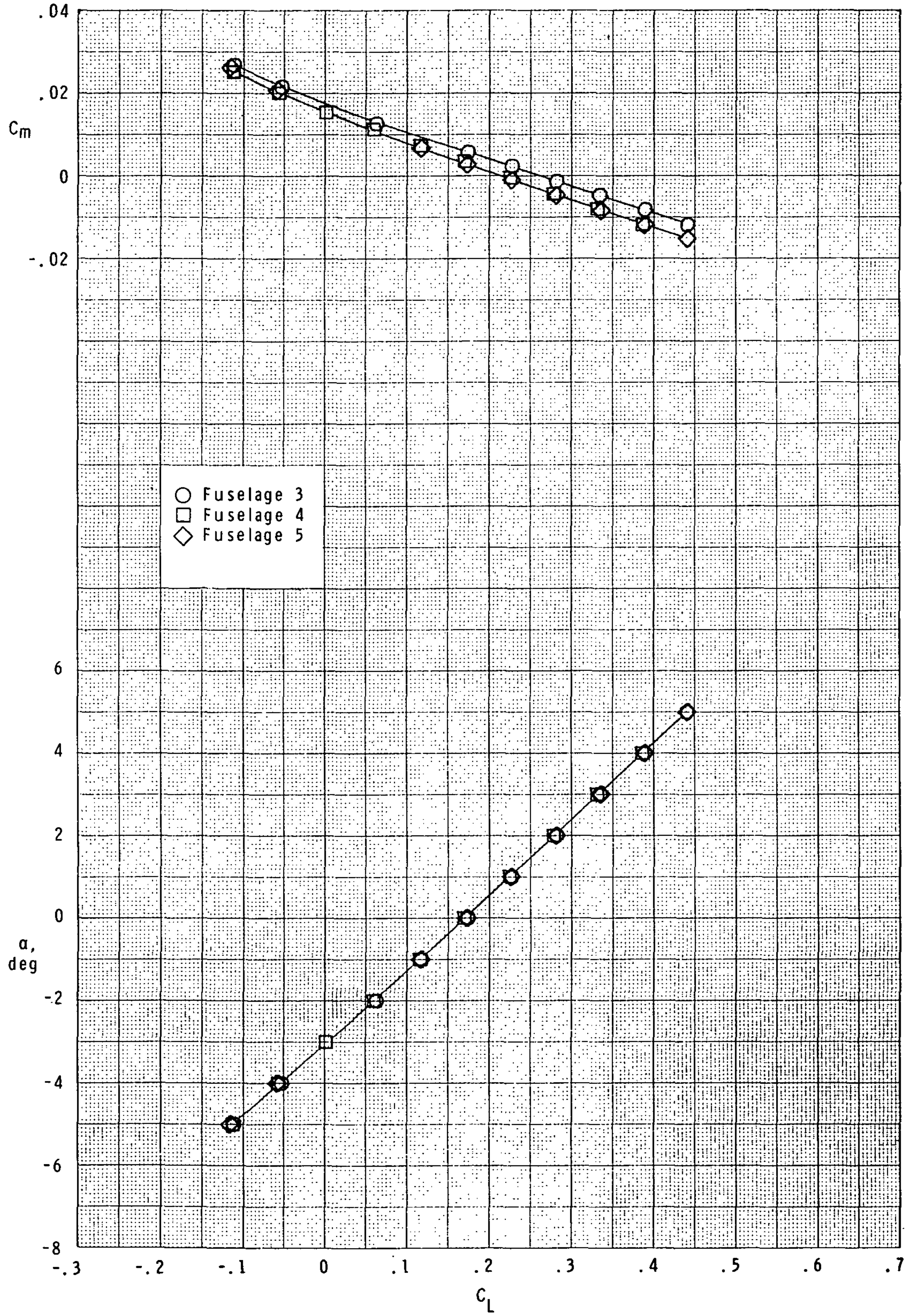

Figure 5.- Effect of fuselage area shift.

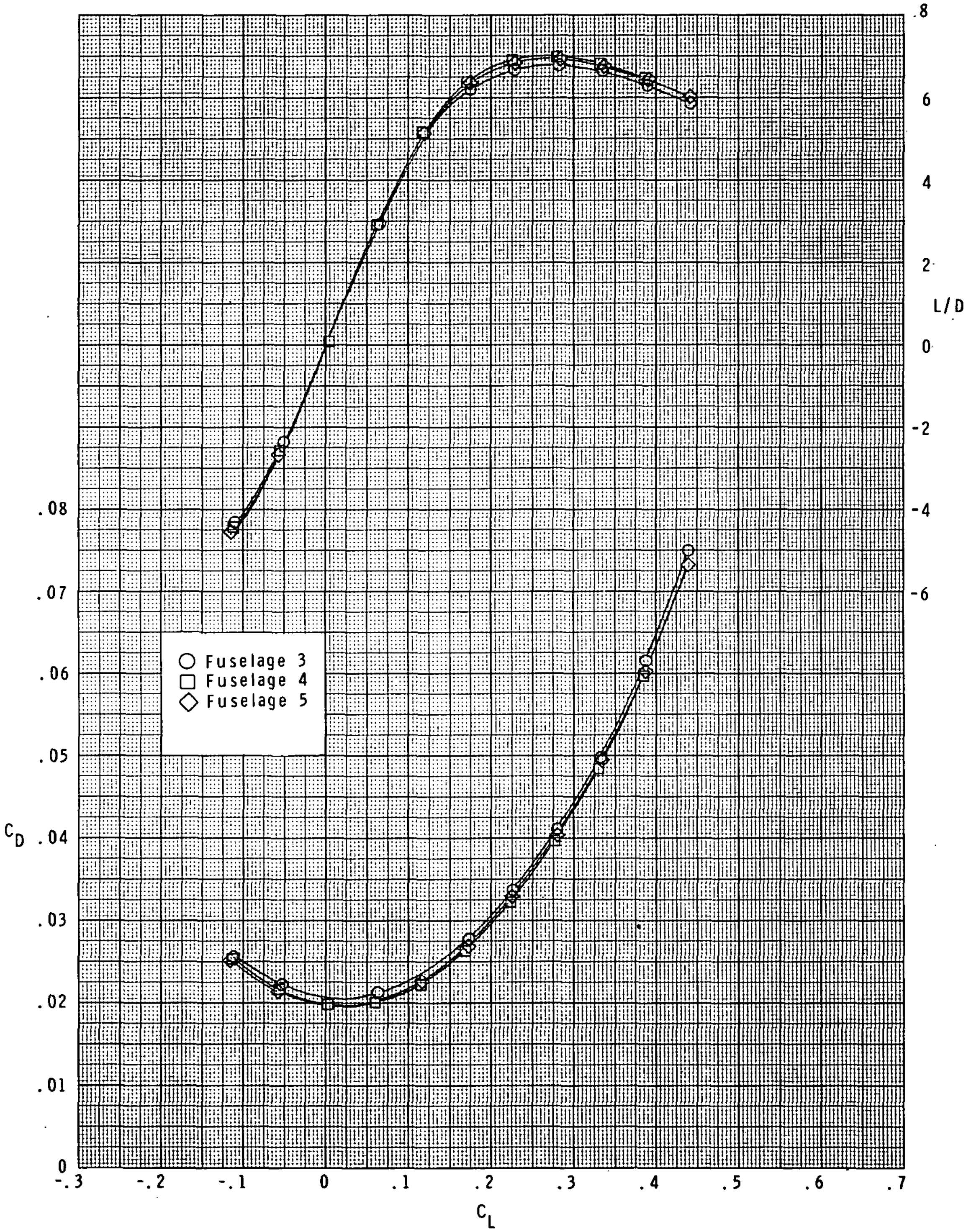

Figure 5.- Concluded.

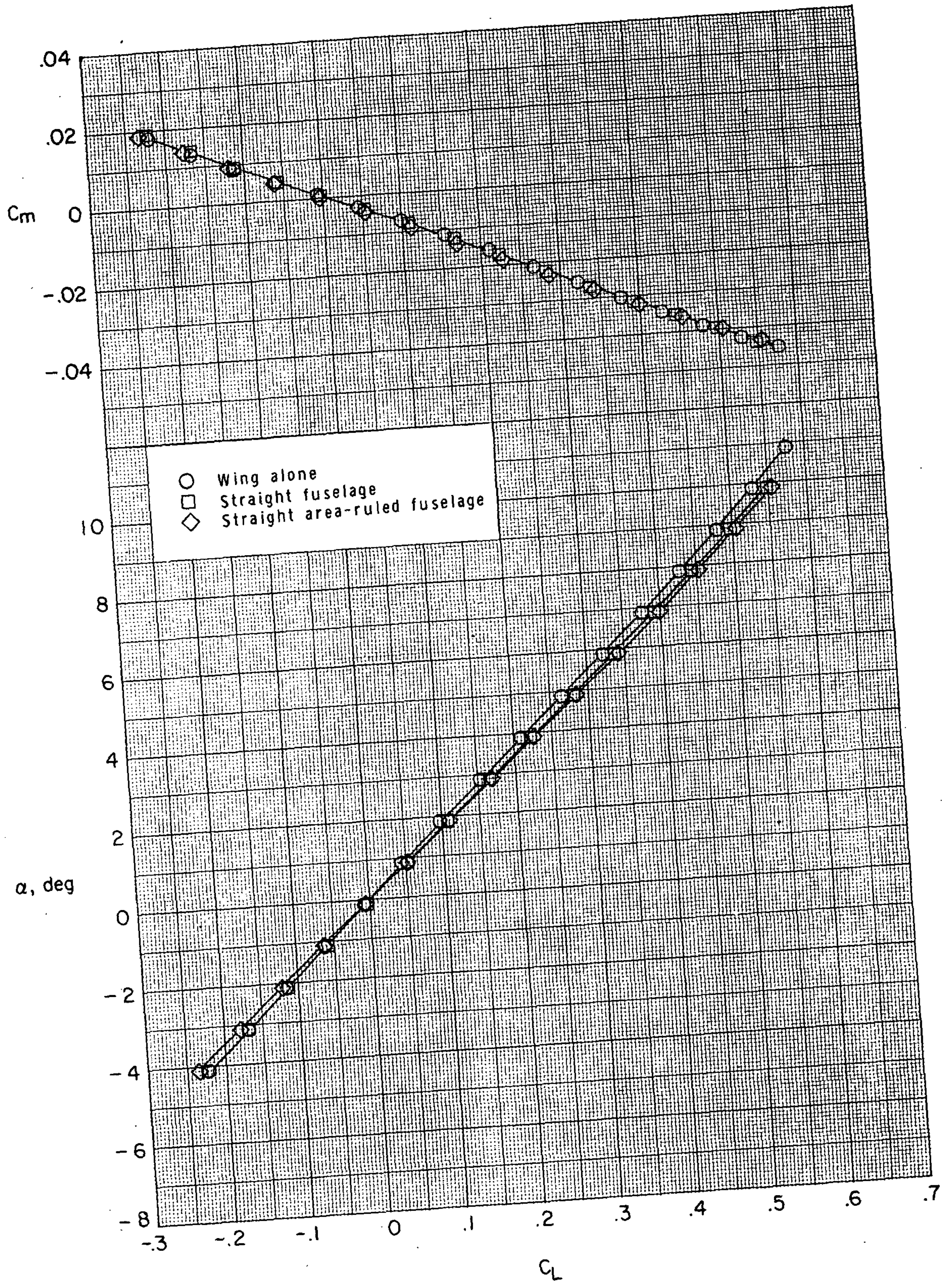

Figure 6.- Effect of area rule on flat wing bodies.

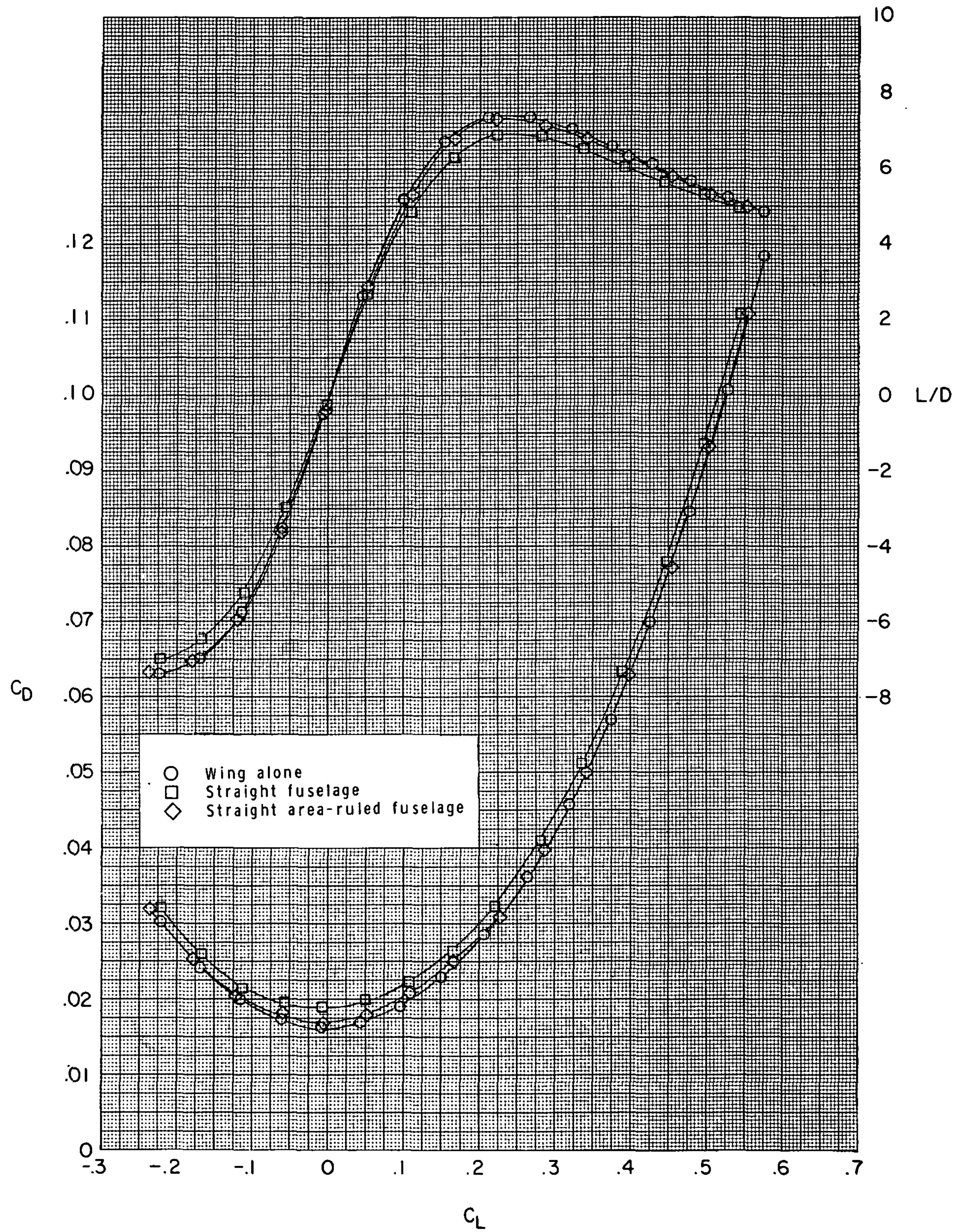

Figure 6.- Concluded.

"The aeronautical and space activities of the United States shall be conducted so as to contribute . . . to the expansion of human knowledge of phenomena in the atmosphere and space. The Administration shall provide for the widest practicable and appropriate dissemination of information concerning its activities and the results thereof."

—NATIONAL AERONAUTICS AND SPACE ACT OF 1958

NASA SCIENTIFIC AND TECHNICAL PUBLICATIONS

TECHNICAL REPORTS: Scientific and technical information considered important, complete, and a lasting contribution to existing knowledge.

TECHNICAL NOTES: Information less broad in scope but nevertheless of importance as a contribution to existing knowledge.

TECHNICAL MEMORANDUMS: Information receiving limited distribution because of preliminary data, security classification, or other reasons. Also includes conference proceedings with either limited or unlimited distribution.

CONTRACTOR REPORTS: Scientific and technical information generated under a NASA contract or grant and considered an important contribution to existing knowledge.

TECHNICAL TRANSLATIONS: Information published in a foreign language considered to merit NASA distribution in English.

SPECIAL PUBLICATIONS: Information derived from or of value to NASA activities. Publications include final reports of major projects, monographs, data compilations, handbooks, sourcebooks, and special bibliographies.

TECHNOLOGY UTILIZATION PUBLICATIONS: Information on technology used by NASA that may be of particular interest in commercial and other non-aerospace applications. Publications include Tech Briefs, Technology Utilization Reports and Technology Surveys.

Details on the availability of these publications may be obtained from:

SCIENTIFIC AND TECHNICAL INFORMATION OFFICE

NATIONAL AERONAUTICS AND SPACE ADMINISTRATION

Washington, D.C. 20546